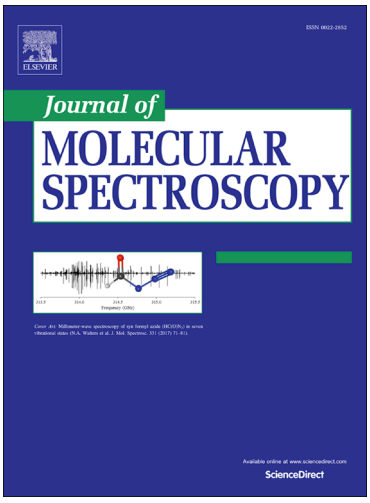

Hyperfine Analysis of the (2, 0) [18.3]3-$X^3\Delta_3$ Transition of Cobalt Monoboride

J.M. Dore, A.G. Adam, D.W. Tokaryk, C. Linton

PII: S0022-2852(19)30085-2
DOI: https://doi.org/10.1016/j.jms.2019.04.011
Reference: YJMSP 11145

To appear in: *Journal of Molecular Spectroscopy*

Received Date: 27 March 2019
Revised Date: 24 April 2019
Accepted Date: 27 April 2019

Please cite this article as: J.M. Dore, A.G. Adam, D.W. Tokaryk, C. Linton, Hyperfine Analysis of the (2, 0) [18.3]3-$X^3\Delta_3$ Transition of Cobalt Monoboride, *Journal of Molecular Spectroscopy* (2019), doi: https://doi.org/10.1016/j.jms.2019.04.011

Hyperfine Analysis of the (2, 0) [18.3]3-$X^3\Delta_3$ Transition of Cobalt Monoboride.

J.M. Dore and A.G. Adam
Department of Chemistry and Centre for Laser, Atomic, and Molecular Sciences, University of New Brunswick, Fredericton, New Brunswick E3B5A3.

D.W. Tokaryk and C. Linton
Department of Physics and Centre for Laser, Atomic, and Molecular Sciences, University of New Brunswick, Fredericton, New Brunswick E3B5A3.

Abstract:
High-resolution laser-induced fluorescence spectra of the (2, 0) [18.3]3-$X^3\Delta_3$ transition of cobalt monoboride (CoB) have been recorded. We report updated rotational parameters for both the [18.3]3 (v'=2) and $X^3\Delta_3$ (v''=0) states of $Co^{11}B$, as well as newly determined hyperfine interaction parameters. The observed hyperfine splitting is mainly due to the nuclear spin of ^{59}Co (I=7/2, μ/μ_N =4.627); the ^{11}B (I=3/2, μ/μ_N = 2.689) interaction only results in broadening of the individual hyperfine transitions. The magnetic hyperfine constants help confirm the ground state electronic configuration, $(8\sigma)^2(3\pi)^4(1\delta)^3(9\sigma)^1$, and provide more insight into the configurational mixing in the excited state.

1. Introduction

Transition metal (TM) borides are regarded as refractory compounds and possess many remarkable physical properties such as their exceptional corrosion resistance, super hardness (ReB_2) [1], and superconducting capability (MgB_2) [2]. As electrical conductors, they often show marked superiority to their parent metals. Many TM borides are known to be good catalysts for hydrogenation of alkenes and alkynes, reduction of nitrogenous functional groups, and deoxygenation reactions [3]. Recently, and pertinent to this work, cobalt boride solid and thin films received special attention because of their ability to catalyze the production of hydrogen in the hydrolysis of sodium borohydride solution [4, 5]. The use of CoB as a catalyst provides a steady control of the hydrogen production rate during the hydrolysis of sodium borohydride solution. All of these intriguing chemical and physical properties prompt further investigation into the chemical bonding and electronic structure of TM borides.

An effective way to resolve the rotational and hyperfine structure in diatomic molecules is to study their gas-phase optical spectra at high resolution. Rotational analysis provides insight into the chemical bonding via the bond length, and it identifies the nature of the electronic states involved via identification of the first rotational transitions in each branch [6]. The hyperfine structure is a sensitive probe which reveals information about the valence electrons and their electronic configuration. This information in turn enables us to understand the nature of more complex molecules containing TM atoms, and the properties of bulk materials containing them.

As far as TM monoborides are concerned, experimental and theoretical studies have been limited mostly to those in groups 9 and 10: CoB [7], RhB [8,9], IrB [10,11], NiB [12], PdB [13], PtB [14] and RuB [15]. Of those 7 TM borides, only IrB and NiB have had their hyperfine structure analysed. In this paper we are focused on analyzing the hyperfine structure of the (2, 0) [18.3]3-$X^3\Delta_3$ transition of CoB. Tzeli and Mavridis [16] have performed theoretical calculations on the ground state of CoB, and predict that the ground state is $X^3\Delta_i$, with an equilibrium bond length r_e=1.700 Å and a vibrational frequency ω_e=708 cm^{-1}. Experimentally, Ng et al. [7] used laser-induced fluorescence (LIF) spectroscopy to

observe and identify four electronic systems of CoB in the 495 – 560 nm range, $[18.1]^3\Pi_2$-$X^3\Delta_3$, $[18.3]^3\Phi_3$-$X^3\Delta_3$, [18.6]3-$X^3\Delta_3$ and [19.0]2-$X^3\Delta_3$. Their analysis determined a bond length of r_0''=1.705 Å and a vibrational separation of $\Delta G_{1/2}''$=731.7 cm^{-1} which compares reasonably well to the values calculated by Tzeli and Mavridis [16]. In this study, we confirmed the ground state as the Ω = 3 component of an inverted $^3\Delta$ state, we improved upon the existing rotational analysis by using high-resolution spectroscopy, and we determined the magnetic hyperfine constants of the [18.3]3 v'=2 and $X^3\Delta_3$ v''=0 states, providing more insight into the ground and, to a lesser extent, excited state electronic configurations. This allows for a good comparison of CoB with the previously studied isovalent molecule IrB [10].

2. Experimental

The molecular production scheme is the same as that used in previous studies [17], therefore only a brief description of the relevant experimental details for obtaining the CoB spectrum is presented here. A slowly rotating and translating cobalt target rod was ablated with ~4 mJ of 355 nm radiation from a Nd:YAG laser to vaporize Co atoms. The hot metal atoms were then reacted with a 1% gas mixture of diborane (B_2H_6) seeded in a helium carrier gas pulsed through a molecular beam valve in order to produce the desired CoB species. The reactant gas mixture passed through a short expansion channel into a high vacuum chamber producing a molecular beam. The molecular jet was then interrogated by a probe laser approximately 5 cm downstream from the jet orifice. The probe laser used for low-resolution survey scans and dispersed fluorescence spectra was a Lumonics HD-500 dye laser pumped by a Nd:YAG laser. For the high-resolution spectra, a Coherent 699-21 cw-ring dye laser pumped by a 488 nm beam from an argon ion laser was used. Coumarin 521 dye was used to provide a lasing wavelength near 520 nm from the cw-ring dye laser, and ~300 mW of output power was obtained.

LIF was collected orthogonal to both the molecular beam and the probe laser beam and was imaged on the entrance slit of a 0.25 m monochromator. For the high-resolution spectra, 2 mm slits were inserted in the monochromator to reduce background noise from laser scatter and the ablation plasma. In order to increase the signal-to-noise ratio, a back-reflecting mirror was installed to redirect the laser beam back through the apparatus. The light passing through the monochromator was detected with a photomultiplier tube, pre-amplified (SRS SR445 DC-300 MHz amplifier), then connected to a photon counter (SRS SR400 two-channel gated photon counter) to record the spectrum. Simultaneously, an iodine spectrum was collected by LIF in order to calibrate the spectral data to I_2 line positions [18]. Interpolation between iodine peaks was achieved by simultaneously recording the transmission of two etalons, which had a free spectral range of ~150 MHz and ~1200 MHz. The 1200 MHz etalon was temperature- and pressure-stabilized and was used mainly to observe if there were any laser mode hops during the scan. The 150 MHz etalon was thermally stabilized and used to calibrate the observed transmission fringes to the measured I_2 spectral features in wavenumber (cm^{-1}).

Typical linewidths of unblended high-resolution spectral lines from our apparatus are ~150 MHz (FWHM) due to residual Doppler broadening. In the present CoB spectra, however, linewidths are on the order of 300 MHz due to unresolved hyperfine structure of the ^{11}B nucleus (I=3/2).

3. Observations and Analysis

Low-resolution LIF spectra obtained using the pulsed-dye laser showed the same CoB transitions observed by Ng et al. [7]. As the CoB signal was weak, only the $^{59}Co^{11}B$ isotopologue was observed.

The (2, 0) band of the [18.3] $^3\Phi_3$-$X^3\Delta_3$ system at ~19200 cm^{-1} was, as in the previous work (Ref. [7] Fig. 3), the most intense transition we observed, so this band was chosen for the high-resolution study. Dispersed fluorescence (DF) spectra showed a ground state vibrational frequency $\Delta G_{1/2} \approx 730$ cm^{-1} in agreement with the value previously obtained $\Delta G_{1/2}$=731.7 cm^{-1} [7] and is further confirmation that CoB molecules were being produced

In the high resolution spectrum of the (2, 0) band, 16 different rotational transitions, P(4)-P(9), Q(3)-Q(7) and R(3)-R(7), were observed, all showing resolved hyperfine structure due to the nuclear spin of ^{59}Co (I=7/2) which splits each rotational level into 8 hyperfine levels labelled by the *F* quantum number. Hyperfine structure due to boron (I=3/2) was unresolved and only contributed to line broadening. Initial analysis of the (2, 0) band showed, as previously reported [7], that the first rotational transitions in each band are P(4), Q(3) and R(3) confirming that both the ground and excited states have Ω=3. The ground state has already been established experimentally [7] and theoretically [16] as $^3\Delta_3$. Based on intensity and configuration considerations, the transition was previously labelled as $^3\Phi_3$-$X^3\Delta_3$ [7]. We find the intensity distribution typical of a $\Delta\Omega = 0$ transition and, as there is a strong possibility of configurational mixing in the excited state, we prefer to assign it with its Ω value in a Hund's case (c) coupling scheme and label the electronic transition as [18.3]3-$X^3\Delta_3$.

The analysis of the (2, 0) band was conducted in stages, starting with the rotational analysis and then moving into the study of hyperfine transitions. The molecular constants from the final fit, which were obtained using PGOPHER [19], and the comparison with previous values [7] are shown in Table 1. The ground state appears normal and unperturbed and the rotational structure was well described with just the *B* rotational constant. The centrifugal distortion constant *D*, however, was well determined and included in the final fit. For the upper state, even though only the lowest 6 rotational levels were observed, the addition of *D* and *H* constants was required to adequately describe the rotational structure and they significantly improved the quality of the fit. Both *D* and *H* were negative and 2 orders of magnitude larger than normal indicating that, although there were no obvious signs of local perturbations, the [18.3]3 state is affected by interactions with other neighbouring states. Comparison of the rotational constants of $Co^{11}B$ with those from Ng et al. [7] shows that the higher resolution results have improved precision by an order of magnitude. The newly calculated ground state bond length r_0''=1.708 Å, still compares well with r_e''=1.700 Å and r_0''=1.705 Å calculated by Tzeli and Mavridis [16] and Ng et al. [7], respectively.

The hyperfine structure was well resolved and the eight intense $\Delta F = \Delta J$ transitions were easily identified in each rotational transition. In addition, weaker satellite transitions with $\Delta F \neq \Delta J$ were observed, providing direct measurements of the hyperfine splittings in each state. This enabled a preliminary calculation of the hyperfine constants, h_Ω' and h_Ω'' (see eqs. 1 – 3 below) which were then used as starting values in the final fit. Figure 1 shows the observed (top) and calculated (bottom) spectra of the R(5) transition. The 8 main $\Delta F = \Delta J = +1$ lines are intense and well resolved. The calculated positions of the $\Delta F = 0$ lines are labelled, but only the F′=8.5 - F″=8.5 satellite line is clearly resolved on the low frequency side of the main transitions while the others are overlapped with and appear as shoulders on the main lines. Fig. 2 shows observed and calculated spectra of the P(4) and P(5) transitions in which the $\Delta F = 0$ transitions are separated from and at higher frequency than the main $\Delta F = -1$ lines but are too closely spaced to be completely resolved.

The electric quadrupole interaction made a negligible contribution to the fit, therefore, the hyperfine energy is composed mainly of the magnetic hyperfine interactions. To a first approximation, the magnetic hyperfine energy W_{mhf} is given by the diagonal term in the hyperfine matrix:

$$W_{mhf} = \frac{h_\Omega \Omega C}{(2J(J+1))} \quad (1)$$

where $$C = [F(F+1) - J(J+1) - I(I+1)] \quad (2)$$

and $$h_\Omega = a\Lambda + \left(b_f + {}^{2c}/_{3}\right)\Sigma, \quad (3)$$

where a, b_f and c are the Frosch and Foley hyperfine parameters [20]. The PGOPHER program [19] was used for fitting and spectral simulation, enabling us to extend assignment of the hyperfine transitions. The weighted fit consisted of 128 optical transitions from $^{59}Co^{11}B$ and reproduced the observed data to within an average standard deviation of 0.0010 cm^{-1}. Transitions were weighted based on the width of the peak at half-maximum (FWHM). Those transitions with broader peaks, either due to overlap or unresolved hyperfine splitting from the ^{11}B nucleus, were weighted less in the final fit than the peaks that had well-defined frequencies. The molecular constants obtained from the fit are presented in Table 1. The transitions used in the fit are supplied in the supplementary material, as well as the residuals from the fit.

Table 1. Molecular constants determined from the analysis of the [18.3]3-$X^3\Delta_3$ (2, 0) band of CoB.

	This Work		Previous Work [7]	
Parameter[a]	$X^3\Delta_3$	[18.3] 3	$X^3\Delta_3$	[18.3] $^3\Phi_3$
T_v	0 (fixed)	19159.24797 (48)[b]	0 (fixed)	19160.88 (3)[b]
B_v	0.622716 (20)	0.470335 (54)	0.6254 (3)	0.4782 (3)
$10^6 D_v$	1.45 (22)	-63.5 (1.6)	-	-
$10^8 H_v$	-	-37.8 (1.4)	-	-
h_3	0.094812 (76)	0.059627 (87)	-	-
$10^5\ h_{3D}$	4.90 (46)	-2.52 (49)	-	-
r_v (Å)	1.7083	1.9656	1.705	1.949

[a]All parameters are in units of cm^{-1} unless otherwise stated.
[b]The difference in the band origin can be attributed to PGOPHER using slightly different matrix elements to determine the constant, and due to different methods of calibration.

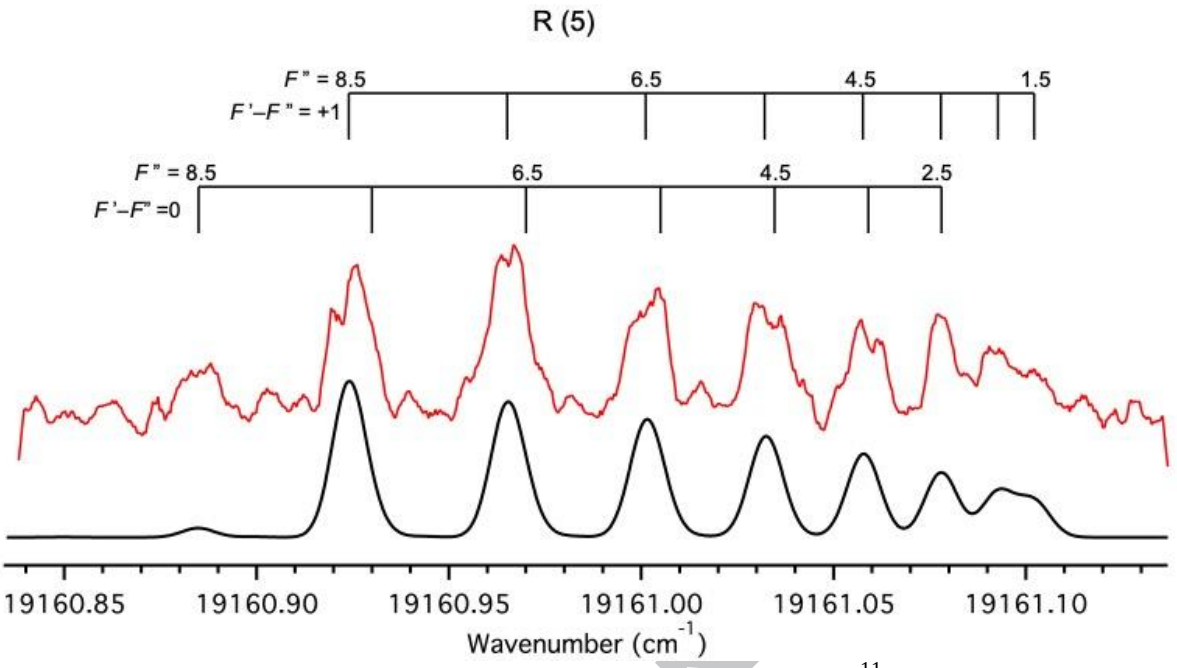

Figure 1. Hyperfine splitting of the R(5) rotational transition of $Co^{11}B$. The top trace shows the observed spectrum, and the simulation of the spectrum using PGOPHER is shown on the bottom. Assigned transitions are based on the simulated spectrum from the final fit. A Gaussian width of 0.01 cm^{-1} and rotational temperature of 35 K were used to obtain the simulated spectrum.

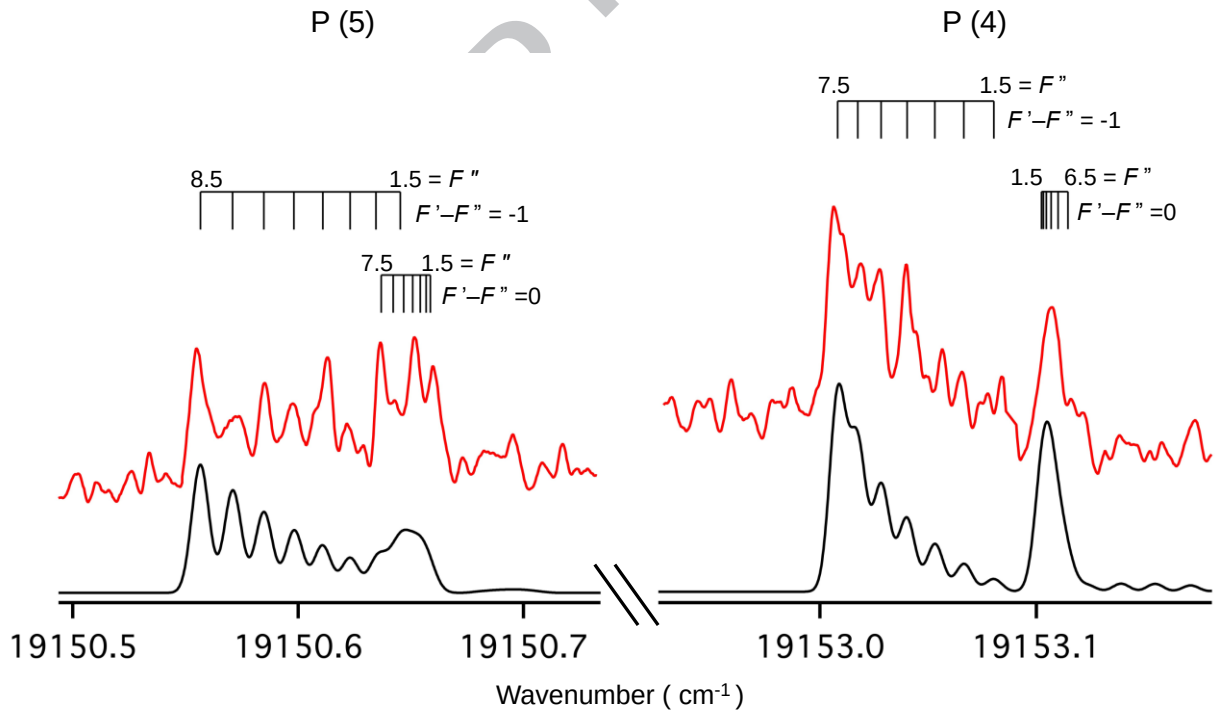

Figure 2. Hyperfine splitting pattern of the P(4) and P(5) rotational transitions. The observed spectra are located on top, and the bottom spectra displays the PGOPHER simulations. Assigned transitions are predicted based on the final fit of CoB. The spectra show the opposing trend of the $\Delta F=\Delta J$

and satellite transitions in P(4) and the reversal of the hyperfine pattern in the $\Delta F \neq \Delta J$ series going from P(4)-P(5).

4. Discussion

Only the (2, 0) band of the [18.3]3-$X^3\Delta_3$ electronic transition of the $Co^{11}B$ isotopologue was analyzed because other bands and those of the $Co^{10}B$ isotopologue were too weak. Molecular parameters of isotopic molecules can, however, be calculated through the mass dependence relationship, $\rho = (\mu/\mu_i)^{1/2}$, where μ and μ_i are the reduced masses of $Co^{11}B$ and $Co^{10}B$, respectively.

$$B_v\,(Co^{10}B) = B_v\,(Co^{11}B) * \rho^2 \qquad (4)$$

Using Eq. (4), the calculated rotational constants for $Co^{10}B$ are B_0"=0.67517 cm^{-1} and B_2'=0.50990 cm^{-1}, where ρ^2 =1.083845. This compares well to the experimentally derived ratio ρ^2=1.080256 from Ng and co-worker's data [7].

The ground state electronic configuration of CoB as discussed in Ref. [7] is:

$(8\sigma)^2(3\pi)^4(1\delta)^3(9\sigma)^1 \rightarrow X^3\Delta_i$ and $a^1\Delta$

Table 2 lists the many excited electronic states from various possible excited electronic configurations arising from a one-electron excitation from the ground electronic configuration (Label A).

Table 2. Excited/ground state electronic configurations of CoB.

Label	Molecular orbital occupancies						Configuration	States
	8σ	3π	1δ	9σ	4π	10σ		
A	2	4	3	1			$\delta^3\sigma$	$X^3\Delta_i$, $a^1\Delta$
B	2	4	3		1		$\delta^3\pi$	$^3\Phi_i$, $^3\Pi_i$, $^1\Phi$, $^1\Phi$
C	2	4	3			1	$\delta^3\sigma$	$^1\Delta$, $^3\Delta_i$
D	2	4	2	1	1		$\delta^2\sigma\pi$	$^1\Pi$, $^1\Phi$, $^3\Pi$, $^3\Phi$, $^5\Pi$

If we assume that the most likely candidates for transitions to the $X^3\Delta_3$ ground state would be triplet states due to the $\Delta S = 0$ selection rule for dipole-allowed transitions, then the $^3\Phi$ states from configurations B and D and the $^3\Delta$ state from configuration C would be the only states with an $\Omega = 3$ component. Ng et al. [7], based on intensity considerations, assigned the [18.3]3 state as the $^3\Phi_3$ state arising from $\delta^3\pi$ configuration B which resulted from excitation of an electron from the 9σ to the 4π orbital. Their intensity argument is not convincing as the intensity distribution is consistent with a $\Delta\Omega = 0$ transition and, as pointed out in Ref. [7], there is a strong possibility of configurational mixing and the possibility of contributions to the excited state from configurations C and D cannot be ruled out.

From examination of the molecular orbital energy level diagram for CoB in Ref. [7] Figure 5, the 1δ molecular orbital (MO) is entirely Co 3dδ. The 9σ MO is Co 4sσ mixed with some B 2pσ and possibly a small contribution from Co 4dσ. The 4π MO is primarily Co 3dπ mixed with some B 2pπ and the 10σ MO is Co 3dσ possibly mixed with some Co 4pσ and B 2pσ. The hyperfine structure might

provide a way to distinguish between the possible configurations.

As only a single spin-orbit component of each state was observed, only h_Ω could be determined as it was not possible to determine any of the individual Frosch and Foley magnetic hyperfine parameters. Approximate values of these parameters can be estimated from atomic hyperfine parameters and the resulting calculated h_Ω compared with the experimentally determined values. The magnetic hyperfine parameters, *a*, b_f, and *c* can be estimated using atomic parameters through the following expressions:

$$a/Hz = \left(\frac{\mu_0}{4\pi h}\right) g_e g_N \mu_B \mu_N \frac{1}{\Lambda} \left\langle \Lambda \left| \sum_i \frac{l_{zi}}{r_i^3} \right| \Lambda \right\rangle_l , \qquad (5)$$

$$b_F/Hz = \left(\frac{\mu_0}{4\pi h}\right)\left(\frac{8\pi}{3}\right) g_e g_N \mu_B \mu_N \frac{1}{\Sigma} \langle \Lambda\Sigma | \sum_i s_{zi} \delta_i(r) | \Lambda\Sigma \rangle_s , \qquad (6)$$

$$c/Hz = \left(\frac{\mu_0}{4\pi h}\right)\frac{3}{2} g_e g_N \mu_B \mu_N \frac{1}{\Sigma} \left\langle \Lambda\Sigma \left| \sum_i s_{zi} \frac{(3\cos^2\theta_i - 1)}{r_i^3} \right| \Lambda\Sigma \right\rangle_s , \qquad (7)$$

where $g_N = \mu/I$, l_{zi} and s_{zi} are orbital and spin angular momentum operators for the *i*th electron, δ(r) is a Dirac delta function, and *r* and θ are polar coordinates; the subscripts *l* and *s* indicate different averages which allow for relativistic effects. δ(r) is essentially the electron density at the nucleus which is only nonzero for sσ molecular orbitals.

The magnetic hyperfine matrix elements for a configuration with a single vacancy are equivalent to those for a configuration with a single electron. The configurations in Table 2 are, for calculation purposes, reduced to A: 1δ9σ - $^3\Delta_i$, B: 1δ3π - $^3\Phi_i$, C: 1δ10σ - $^3\Delta_i$. Configuration D remains as 1δ^{2}9σ4π - $^3\Phi$. From eq. 3, the expressions for h_Ω become

$$\text{For } {}^3\Delta_3\text{:-}\ \Lambda = 2, \Sigma = +1, h_3 = 2a + (b_F + 2c/3); \quad \text{For } {}^3\Phi_3\text{:-}\ \Lambda = 3, \Sigma = 0, h_3 = 3a \qquad (8)$$

The following values are used in the calculations:
For ^{59}Co:- I = 7/2, μ = 4.63μ_N [21], $g_N = 1.322\mu_N$, $\langle r_i^{-3} \rangle$ = 6.710 a.u^{-3}, δ(r) = $|\psi^2(0)|$ = 5.233 [22].
For ^{11}B:- I = 3/2, μ = 2.689μ_N [21], $g_N = 1.793\mu_N$, $\langle r_i^{-3} \rangle$ = 0.929 a.u^{-3}, δ(r) = $|\psi^2(0)|$ = 1.775 [22].

Ground State, Co 3dδ9σ:- If the 9σ orbital is 100% Co 4sσ, we obtain *a*(Co)=0.02823 cm^{-1}, b_F(Co)=0.0922 cm^{-1} and *c*(Co)=-0.0121 cm^{-1} giving h_3"(Co)=0.1406 cm^{-1}. The parameter, *a*, will remain unchanged irrespective of the composition of the 9σ MO. If the 9σ orbital is B 2pσ, then b_F(Co) = 0, *c*(Co) = -0.0121 cm^{-1} and h_3''(Co)=0.0485 cm^{-1}. The experimentally determined value, h_3"(Co)=0.0949cm^{-1} could be obtained if the 9σ MO were a mixture of 55% Co4sσ and 45% B2pσ. This would also give a boron hyperfine constant of h_3''(B)=0.0014 cm^{-1}. The magnitude of h_3''(B) would not be sufficient to resolve the boron hyperfine structure but could contribute to the broadening of the lines. A similar calculation for Co3dσ would give b_F(Co)=0, *c*(Co) =0 and h_3"(Co)=0.05646 cm^{-1}. This MO is expected to make, at best, only a small contribution to the 9σ MO. Whatever the precise nature of the ground state configuration, the hyperfine structure suggests that the 9σ MO is a mixture with significant contributions from both cobalt and boron σ orbitals.

Excited [18.3]3 state:- There are three possible electronic configurations listed in Table 2 as B, C and D. The experimentally determined hyperfine constant is h_3'=0.059872 cm^{-1} and there are

numerous possible calculated h_3' values depending on the composition of the 9σ, 4π and 10σ MOs. The following values of h_3'(Co) are obtained. **Configuration B $^3\Phi_3$:-** Co3dδ^{3}3dπ, h_3'(Co)=0.0846 cm^{-1}; Co3dδ^{3}B2pπ, h_3'(Co)=0.0564 cm^{-1} and h_3'(B)=0.0081 cm^{-1}. **Configuration C $^3\Delta_3$:-** Co3dδ^{3}3dσ, h_3'(Co)=0.0564 cm^{-1}; Co3dδ^{3}4pσ, h_3'(Co)=0.0596 cm^{-1}; Co3dδ^{3}B2pσ, h_3'(Co)=0.0485 cm^{-1} and h_3'(B)=0.0081 cm^{-1}. **Configuration D $^3\Phi_3$:-** Co3dδ^{2}9σ3dπ, h_3'(Co)=0.0846 cm^{-1}; Co3dδ^{2}9σB2pπ, h_3'(Co)=0.1128 cm^{-1} and h_3'(B)=-0.0081 cm^{-1}. Ng et al. [7] tentatively assigned the excited state as the $^3\Phi_3$ state arising from configuration B. Based on the above calculations, this would require the 4π MO to be almost entirely due to the boron 2pπ atomic orbital which is not realistic. For the other $^3\Phi_3$ state from configuration D, the hyperfine parameter will be too high whatever the composition of the 4π MO. For the $^3\Delta_3$ state from configuration C, the hyperfine parameters are close to the experimental value with the 10σ MO composed of cobalt 3dσ and/or 4pσ with little or no contribution from boron 2pσ. It should be pointed out that the above calculations are relying on atomic parameters which may not all be very precise, but the present calculations suggest that the primary contribution to the [18.3]3 state might come from a $^3\Delta_3$ state which is probably mixed with some $^3\Phi_3$ character. In this case, the transition will be completely allowed as it will satisfy the $\Delta\Sigma = 0$ selection rule. The calculations also show that any boron hyperfine parameters will be very small.

A comparison of the main properties of Group 9 transition metal monoborides is presented in Ref. [7] Table II. This did not include hyperfine parameters and it is interesting to compare these for the ground states of CoB and IrB, both of which share the same electronic state and configuration, $\delta^3\sigma \rightarrow X^3\Delta_3$. Calculations, similar to those above, for ^{193}Ir^{11}B (I=3/2 for ^{193}Ir) give h_3''(Ir)=0.0288 cm^{-1} for the Ir5dδ^{3}6sσ configuration which is in excellent agreement with the observed experimental value of 0.029 cm^{-1} [10]. Not too much weight should be attached to the closeness of this agreement as the experimental data were imprecise width measurements of a few lines broadened by unresolved hyperfine structure and the atomic data are also not precise. The calculations, however, do indicate that boron makes only a small contribution to the hyperfine structure in IrB. The previous research [10] described the hyperfine splitting in the IrB spectra as due mainly to the ^{11}B nuclear spin I=3/2, but the calculation from the configuration indicates that this is clearly incorrect. It seems that, as one moves from CoB to the more massive IrB along the Group 9 transition metal monoborides, the valence σ orbital becomes less of an admixture of atomic orbitals towards a larger composition of the transition metal's valence sσ orbital. This could be an indication that, as the energy separation between AOs increases with an increase in principal quantum number, n, there is less of an admixture when forming the hybridized MOs.

In summary, the analysis of this first high-resolution spectrum of the [18.3]3-X$^3\Delta_3$ (2, 0) band of CoB has improved the rotational constants by an order of magnitude over those obtained from the previous analysis of lower resolution spectra [7]. In addition, the Co magnetic hyperfine structure was resolved and analysed. Values of the hyperfine parameter, h_3, for both states were determined for different possible configurations using the Frosch – Foley parameters a, b_F, and c which were calculated using atomic hyperfine parameters in Eqs. 5 – 7. The hyperfine parameters were compared with the observed values to try and establish the composition of the molecular orbitals responsible for the observed states. For the ground state, the hyperfine analysis confirmed the configuration 3dδ^{3}9σ where the 9σ orbital is a mixture of Co 4sσ and B 2pσ orbitals. The situation in the excited state was less clear as there were several configurations that would give an $\Omega = 3$ excited state. The calculations of the hyperfine structure showed a preference for the $^3\Delta_3$ state from the 3dδ^{3}10σ configuration where 10σ is

probably a mixture of Co 3dσ and 4pσ orbitals with, at most, a very small contribution from B 2pσ. There may also be some $^3\Phi_3$ state character from configurations B and/or D mixed in. The calculations also show that any boron hyperfine structure will be very small which is consistent with the observation of a slight broadening of the CoB hyperfine lines. The hyperfine structure provides some guidance as to the nature of the electronic states but the calculations are not very precise. There is a real need for high level ab initio calculations to determine the properties of the ground and excited states of CoB.

Acknowledgments:

The work described here was supported by a grant from the Natural Sciences and Engineering Research Council of Canada. The authors would also like to thank Joyce MacGregor for her laser expertise and help with the experiments.

References:

1. H.-Y. Chung, M. B. Weinberger, J. B. Levine, A. Kavner, J.-M. Yang, S. H. Tolbert, R. B. Kaner, Science, 316 (2007), pp. 436-439.
2. H. J. Choi, D. Roundy, H. Sun, M. L. Cohen, S. G. Louie, Nature, 418 (2002), pp. 15-17.
3. B. Ganem, J. O. Osby, Chem. Rev., 86 (1986), pp. 763-780.
4. P. Krishnan, S. G. Advani, A. K. Prasad, Appl. Catal. B Environ., 86 (2009), pp. 137-144.
5. C. C. Yang, M. S. Chen, Y. W. Chen, Int. J. Hydrogen Energy, 36(2011), pp. 1418-1423.
6. G. Herzberg, Spectra of diatomic molecule, Van Nostrand, New York, 1950.
7. Y. W. Ng, H. F. Pang, A. S.-C. Cheung, J. Chem. Phys., 135 (2011), pp. 1-6.
8. P. K. Chowdhury, W. J. Balfour, J. Chem. Phys., 124 (2006), pp. 216101.
9. P.K Chowdhury, W. J. Balfour, Mol. Phys., 105 (2007), pp. 1619-1624.
10. J. Ye, H. F. Pang, A. M.-Y. Wong, J. W.-H. Leung, A. S.-C. Cheung, J. Chem. Phys., 128 (2008), pp. 154321.
11. H. F. Pang, Y. W. Ng, Y. Xia, A. S.-C. Cheung, Chem. Phys. Lett., 501 (2011), pp. 257-262.
12. E. S. Goudreau, A. G. Adam, D. W. Tokaryk, C. Linton, J. Mol. Spectrosc., 314 (2015), pp. 13-18.
13. Y. W. Ng, H. F. Pang, Y. Qian, A. S.-C. Cheung, J. Phys. Chem., 116 (2012), pp. 11568-11572.
14. Y. W. Ng, Y. S. Wong, H. F. Pang, A. S.-C. Cheung, J. Chem. Phys., 137 (2012), pp. 124302.
15. N. Wang, Y. W. Ng, A. S.-C. Cheung, Chem. Phys. Lett., 547 (2012), pp. 21-23.
16. D. Tzeli, A. Mavridis, J. Chem. Phys., 128 (2008), pp. 1-15.
17. A. G. Adam, L. P. Fraser, W. D. Hamilton, M. C. Steeves, Chem. Phys. Lett., 230 (1994), pp. 82-86.
18. (a) S. Gerstenkorn, P. Luc, Atlas du spectre d'absorption de la molécule d'iode Technical Report, Editions du C. N. R. S. Paris, France, 1978;
(b) Rev. Phys. Appl., 14 (1979), pp. 791-794.
19. C. M. Western, Journal of Quantitative Spectroscopy & Radiative Transfer, 186 (2016), pp. 221-242.
20. R. A. Frosch, H. M. Foley, Phys. Rev., 88 (1952), pp. 1337-1349.
21. J.M Brown, A. Carrington, Rotational Spectroscopy of Diatomic Molecules, Cambridge University Press, Cambridge, 2003.
22. J. R. Morton, K. F. Preston, J. Magn. Reson., 30 (1978), pp. 577-582.

Highlights:

- High-resolution spectrum of CoB.
- Fine and hyperfine analysis of the (2, 0) [18.3]3-$X^3\Delta_3$ transition.
- Comparison of experimental hyperfine constants to calculated values from atomic parameters.
- Analysis of excited state configurational mixing.
- Comparison of the ground state hyperfine parameters to those of the isoelectronic species IrB.

Graphical abstract